THE X-RAY HALO OF THE LOCAL GROUP AND ITS IMPLICATIONS FOR MICROWAVE AND SOFT X-RAY BACKGROUNDS

Yasushi Suto[1,2], Kazuo Makishima[1,2], Yoshitaka Ishisaki[1], & Yasushi Ogasaka[3]

[1] *Department of Physics, The University of Tokyo, Tokyo 113, Japan*
[2] *RESCEU (Research Center for the Early Universe), School of Science, The University of Tokyo, Tokyo 113, Japan*
[3] *Institute of Space and Astronautical Science, 3-3-1 Yoshinodai, Sagamihara, Kanagawa 229, Japan*
e-mail: suto@phys.s.u-tokyo.ac.jp, maxima@phys.s.u-tokyo.ac.jp, ishisaki@miranda.phys.s.u-tokyo.ac.jp, ogasaka@astro.isas.ac.jp,

Received 1995 December 26; accepted 1996 January 31

Astrophysical Journal (Letters), in press.

ABSTRACT

Since recent X-ray observations have revealed that most clusters of galaxies are surrounded by an X-ray emitting gaseous halo, it is reasonable to expect that the Local Group of galaxies has its own X-ray halo. We show that such a halo, with temperature $\sim$ 1keV and column density $\sim O(10^{21})\mathrm{cm}^{-2}$, is a possible source for the excess low-energy component in the X-ray background. The halo should also generate temperature anisotropies in the microwave background via the Sunyaev-Zel'dovich effect. Assuming an isothermal spherical halo with the above temperature and density, the amplitude of the induced quadrupole turns out to be comparable to the COBE data without violating the upper limit on the y-parameter. The induced dipole is negligible compared to the peculiar velocity of the Local Group, and multipoles higher than quadrupole are generally much smaller than the observed ones. However non-sphericity and/or clumpiness of the halo will produce a stronger effect. Therefore the gaseous halo of the Local Group, if it exists, will affect the estimate of the primordial spectral index n and the amplitude of the density fluctuations deduced from the *COBE* data.

Subject headings: cosmic microwave background — cosmology: theory — diffuse radiation — Local Group

1. INTRODUCTION

The origin of the X-ray background (XRB) remains one of the most challenging problems in X-ray astrophysics. Figure 1 summarizes the current results on the XRB energy spectra, $I(\varepsilon)$ below 10 keV observed with different satellites. As is known (McCammon & Sanders 1990; Fabian & Barcons 1992), $I(\varepsilon) \sim 10\varepsilon^{-0.4}\mathrm{keV}\cdot\mathrm{s}^{-1}\cdot\mathrm{sr}^{-1}\cdot\mathrm{keV}^{-1}$ is a good empirical fit over the range 3 to 10 keV , where ε denotes X-ray energy in units of keV . Both Einstein IPC (Wu et al. 1991; plotted in diamonds) and Rosat (Hasinger 1992; Shanks et al. 1991; upper-left lines) data suggest a large excess below 2 keV . More recently the Japanese X-ray satellite ASCA (crosses) reported a modest but significant excess soft component below 1 keV relative to the extrapolation of the above power-law fit in the higher energy band (Gendreau et al. 1995). Thus the existence of the soft excess is well established although its amplitude is still somewhat controversial.

Since Galactic absorption becomes important in the soft X-ray energy band, the origin of this excess component allows several possibilities including Galactic sources, extragalactic point-like sources (Hasinger 1992; Shanks et al. 1991), a diffuse thermal component (Wang & MaCray 1993), the accumulation of the thermal bremsstrahlung emission from distant clusters of galaxies (Kitayama & Suto 1996). Cen et al. (1995) found an excess of soft X-ray background below 1 keV from their hydrodynamical simulations which properly incorporate the line emissions as well as the thermal bremsstrahlung emission; the excess is mainly originated from the the low temperature and low density plasma surrounding distant clusters of galaxies since cooler background gas produces much stronger line emissions. Yet another possibility which we propose here is the emission from an X-ray halo of the Local Group (LG). Since the gaseous halos of clusters of galaxies are known to be strong sources of X-rays, it is reasonable to assume that the LG has its own X-ray halo.

2. SUNYAEV-ZEL'DOVICH EFFECT DUE TO THE HALO OF THE LOCAL GROUP

To be more specific, suppose that the LG is associated with a spherical isothermal plasma whose electron number density is given by

$$n_e(r) = n_0 \frac{r_c^2}{r^2 + r_c^2}, \tag{1}$$

where n_0 is the central density and r_c is the core radius. If we are located at distance x_0 off the LG center (Fig. 2), the electron column density at angular separation θ from the direction to the center is

$$N_e(\mu) = \int_0^\infty \frac{n_0 r_c^2 d\xi}{\xi^2 - 2x_0\mu\xi + x_0^2 + r_c^2} = \frac{n_0 r_c^2}{x_0} \frac{1}{\sqrt{a^2 - \mu^2}} \left[\frac{\pi}{2} + \sin^{-1}\left(\frac{\mu}{a}\right) \right], \tag{2}$$

where $\mu \equiv \cos\theta$, and $a \equiv \sqrt{1 + (r_c/x_0)^2}$. In Fig.1 the LG halo contribution to the XRB spectra simulated with the Raymond-Smith model assuming an isothermal plasma temperature $T = 1\mathrm{keV}$, $r_c = 0.15\mathrm{Mpc}$, $x_0 = 0$, $n_0 = 10^{-4}\mathrm{cm}^{-3}$ and 0.3 times solar abundances is also plotted(lower-left histogram). If we add this component to $I(\varepsilon) = 9.6\varepsilon^{-0.4}\mathrm{keV} \cdot \mathrm{s}^{-1} \cdot \mathrm{sr}^{-1} \cdot \mathrm{keV}^{-1}$, the soft excess around 1 keV is explained. Note that it is not our primary purpose here to find the best fit parameters because the single power-law component is simply an extrapolation from the higher energy band and also because the possible Galactic absorption is not taken into account here. Nevertheless it is interesting to see that the LG halo can be a possible origin for the soft excess.

If the X-ray halo of the LG really exists and accounts for the soft excess component in the XRB, it should also produce temperature anisotropies in the cosmic microwave background (CMB) via the Sunyaev-Zel'dovich (SZ) effect (Zel'dovich & Sunyaev 1969; Cole & Kaiser 1988; Makino & Suto 1993; Persi et al. 1995). In the Rayleigh-Jeans regime, the SZ temperature decrement is given by

$$\left(\frac{\delta T}{T}\right)_{\mathrm{sz}}(\mu) = -2\frac{kT}{mc^2}\sigma_{\mathrm{T}} N_e(\mu), \tag{3}$$

where k is the Boltzmann constant, m is the electron mass, c is the velocity of light, and σ_T is the cross section of the Thomson scattering. We compute the multipoles expanded in spherical harmonics:

$$\left(\frac{\delta T}{T}\right)(\theta,\varphi) = \sum_{l=0}^{\infty}\sum_{m=-l}^{l} a_l^m\, Y_l^m(\theta,\varphi). \tag{4}$$

With eqs.(2) and (4), one obtains

$$(a_l^0)_{\rm sz} = -2\sqrt{(2l+1)\pi}\frac{kT}{mc^2}\sigma_{\rm T}\int_{-1}^{1} N_e(\mu)P_l(\mu)\,d\mu, \tag{5}$$

where $P_l(\mu)$ are the Legendre polynomials. Averaging over the sky, the above SZ anisotropies are expected to contribute in quadrature to the CMB anisotropies as

$$\langle\left(\frac{\delta T}{T}\right)^2\rangle = \frac{1}{4\pi}\sum_{l=0}^{\infty}(2l+1)\langle|a_l^m|^2\rangle = \frac{1}{4\pi}\sum_{l=0}^{\infty}(a_l^0)^2_{\rm sz} \equiv \sum_{l=0}^{\infty}(T_{l,\rm sz})^2. \tag{6}$$

The corresponding monopole, dipole and quadrupole anisotropies reduce to

$$T_{0,\rm sz} = \pi\theta_c\,\sigma_{\rm T}\frac{kT}{mc^2}\frac{n_0 r_c^2}{x_0}, \tag{7}$$

$$T_{1,\rm sz} = 2\sqrt{3}\left(1-\frac{r_c}{x_0}\theta_c\right)\sigma_{\rm T}\frac{kT}{mc^2}\frac{n_0 r_c^2}{x_0}, \tag{8}$$

$$T_{2,\rm sz} = \frac{\sqrt{5}\pi}{4}\left[\theta_c - 3\frac{r_c}{x_0} + 3\left(\frac{r_c}{x_0}\right)^2\theta_c\right]\sigma_{\rm T}\frac{kT}{mc^2}\frac{n_0 r_c^2}{x_0}, \tag{9}$$

where $\theta_c \equiv \tan^{-1}(x_0/r_c)$.

The *COBE* FIRAS data (Mather et al. 1994) imply that the Compton y-parameter, y, should be less than 2.5×10^{-5} (95% confidence level). With eq.(7), this upper limit is translated to

$$n_0 r_c^2/x_0 < 1.1\times10^{22}\left(\frac{1.17}{\theta_c}\right)\left(\frac{y}{2.5\times10^{-5}}\right)\left(\frac{1\rm keV}{T}\right)\ {\rm cm}^{-2}. \tag{10}$$

For example taking $r_c = 0.15$Mpc and $x_0 = 0.35$Mpc, the constraint (10) indicates that

$$T_{1,\rm sz} < 3\times10^{-5}\left(\frac{y}{2.5\times10^{-5}}\right), \tag{11}$$

$$T_{2,\rm sz} < 1.3\times10^{-5}\left(\frac{y}{2.5\times10^{-5}}\right). \tag{12}$$

The analysis of the 1st 2 years' *COBE* DMR data (Górski 1994; Górski et al. 1994; Bennett et al. 1994; Wright et al. 1994), on the other hand, yields $T_{1,\rm COBE} = (1.23 \pm 0.09)\times 10^{-3}$, and $T_{2,\rm COBE} = (2.2\pm 1.1)\times 10^{-6}$. Therefore the LG X-ray halo can potentially have significant effect on the quadrupole of the CMB anisotropies, while its effect on dipole is totally negligible compared to the peculiar velocity of the LG with respect to the CMB rest frame.

3. IMPLICATIONS

Primordial density fluctuations with power spectrum $P(k) \propto k^n$ induce CMB anisotropies via the Sachs-Wolfe effect with multipoles (e.g., Peebles 1993)

$$C_l \equiv \langle |a_l^m|^2 \rangle \propto \frac{\Gamma(l+n/2-1/2)}{\Gamma(l-n/2+5/2)}, \tag{1}$$

where $\Gamma(\nu)$ is the Gamma function. Therefore the standard Harrison-Zel'dovich ($n = 1$) spectrum predicts that

$$\frac{l(l+1)C_l}{6C_2} = 1. \tag{2}$$

The analytic expressions for the higher multipoles (eq.[5]) are quite complicated. Instead we have numerically computed $(C_l)_{\rm sz} \equiv (a_l^0)_{\rm sz}^2/(2l+1)$ which are plotted in Fig.3. Clearly the higher multipoles decrease very rapidly with l. Thus even if the CMB quadrupole were contaminated by the SZ effect described here, the higher moments would be relatively free from such an effect and can be interpreted to reflect the true cosmological signature (the octapole may be affected to some extent). Although the contribution of a distant cluster of galaxies to the multipoles is small, its cumulative effect over the high-redshift may be observable in the small-scale CMB anisotropies (Bennett et al. 1993; Makino & Suto 1993; Persi et al. 1995).

In this context it is interesting to note that the *rms* quadrupole amplitude from the *COBE* 2 years' data, $Q_{\rm rms} = (6 \pm 3)\mu$K, is significantly smaller than that expected from

the higher multipoles (Górski 1994; Górski et al. 1994; Bennett et al. 1994; Wright et al. 1994); if one fixes $n = 1$, for instance, the power spectrum fitting using eq.(1) requires that the most likely amplitude should be $Q_{\rm rms-PS} = (18.2 \pm 1.5)\mu$K. It is somewhat common to ascribe the difference to cosmic variance. It is possible, however, to account for it in terms of our model described here, depending on the actual pattern of the primordial temperature fluctuations.

In turn we can constrain the properties of the possible LG halo from the COBE data. This is summarized in Fig. 4. In fact, the parameter range which is required for the LG halo to provide the excess soft component is largely consistent with the current COBE data. In addition, the LG X-ray halo should produce a dipole signature (toward M31 and the opposite direction) in the soft excess component; the flux f plotted in Fig. 1 corresponds to what should be observed at the center of the halo. If we adopt $x_0 = 0.35$Mpc, the flux towards M31 should be $1.27f$ while $0.73f$ for the opposite direction. Such a level of XRB variation is detectable with careful data analysis of, for instance, the ASCA GIS observation. It should be noted that the cooling time of the X-ray halo at the center due to the thermal bremsstrahlung emission is roughtly estimated as

$$t_{cool} \equiv \frac{3n_0kT}{\varepsilon_{ff}} \sim 3 \times 10^{11} \left(\frac{10^{-4}{\rm cm}^{-3}}{n_0}\right) \sqrt{\frac{T}{1{\rm keV}}} \ {\rm years}, \tag{3}$$

where ε_{ff} is the thermal bremsstrahlung emission rate per unit volume for the primordial gas. Since t_{cool} is significantly larger than the age of the universe for the parameters which we are interested in here, such a LG halo is expected to survive for long once it is formed.

Our model described above assumes a fairly idealistic density profile (1). A more realistic profile of the halo including non-sphericity and spatial inhomogeneity in temperature and density will have a stronger effect on the higher multipoles ($l \geq 3$). Therefore one might even probe the properties of the LG halo through the multipoles of the CMB

map. The direct X-ray detection of, or constraints on, the LG halo component is of great importance in deriving the primordial spectral index n and the amplitude of the density fluctuations from the *COBE* data. It is also important to search for the signature of, and/or put constraints on, the LG halo from the direct analysis of the ROSAT and COBE data.

We are grateful to the referee, Renyue Cen, for his pertinent comments on the earlier manuscript of the present *Letter*. We also thank Naoshi Sugiyama for discussions, and Ewan Stewart for a careful reading of the manuscript. This research was supported in part by the Grants-in-Aid by the Ministry of Education, Science and Culture of Japan (07740183, 07CE2002).

REFERENCES

Bennett,C.L. et al. 1993, ApJL, 414, L77

Bennett,C.L. et al. 1994, ApJ, 436, 423

Cen,R., Kang,H., Ostriker,J.P., & Ryu,D. 1995, ApJ, 451, 436

Cole,S. & Kaiser,N. 1988, MNRAS, 233, 637

Fabian,A.C. & Barcons,X. 1992, ARA & A, 30, 543

Gendreau,K.C. et al 1995, Pub.Astron.Soc.Japan., 47, L5

Górski 1994, ApJL, 430, L85

Górski et al. 1994, ApJL, 430, L89

Hasinger, G. 1992, The X-ray Background eds. Barcons, X. & Fabian, A.C., (Cambridge University Press: Cambridge), 229

Kitayama,T. & Suto,Y. 1996, MNRAS, in press.

Makino,N. & Suto,Y. 1993, ApJ, 405, 1

Mather,J.C. et al. 1994, ApJ, 420, 439

McCammon,D. & Sanders, W.T. 1990, ARA & A, 28, 657

Peebles,P.J.E. 1993, Principles of Physical Cosmology (Princeton University Press: Princeton)

Persi,F.M., Spergel,D.N., Cen,R., & Ostriker,J.P. 1995, ApJ, 442, 1

Shanks, T. et al. 1991, Nature, 353, 315

Wang,Q.D., & MaCray,R. 1993, ApJ, 409, L37

Wright,E.L., Smoot,G.F., Bennett,C.L., & Lubin,P.M. 1994, ApJ, 436, 443

Wu,X., Hamilton,T, Helfand,D.J., & Wang, Q. 1991, ApJ, 379, 564

Zel'dovich,Ya.B. & Sunyaev,R.A. 1969, Ap.Sp.Sci., 4, 301

FIGURE CAPTIONS

Figure 1 : XRB spectra observed with different X-ray satellites. The size of the symbols denote the error bars for ASCA (Gendreau et al. 1995; crosses) and Einstein (Wu et al. 1991; diamonds). The Rosat data (Hasinger 1992) are indicated by the region between the two lines in the upper left. The histogram in the lower left indicates the emission from the X-ray halo of the Local Group with $T = 1\mathrm{keV}$, $r_c = 0.15\mathrm{Mpc}$, $n_0 = 10^{-4}\mathrm{cm}^{-3}$ and 0.3 times solar abundances observed at the center of the LG (computed with the Raymond-Smith model). This LG halo model has a total X-ray luminosity of $10^{41}\mathrm{erg}\cdot\mathrm{s}^{-1}$ between 0.5keV and 4keV, and an electron column density of $6 \times 10^{20}\mathrm{cm}^{-2}$. The single power-law component extrapolated from the higher energy band, $I(\varepsilon) = 9.6\varepsilon^{-0.4}\mathrm{keV}\cdot\mathrm{s}^{-1}\cdot\mathrm{sr}^{-1}\cdot\mathrm{keV}^{-1}$, is plotted in the dotted line, while the overall prediction (the Local Group emission plus the power-law component) is plotted in the solid line. The Galactic absorption is not taken into account.

Figure 2 : Assumed geometry of the X-ray halo of the Local Group.

Figure 3 : Multipoles induced by the Sunyaev-Zel'dovich effect of the Local Group halo. The primordial Harrison-Zel'dovich spectrum prediction $l(l+1)C_l/(6C_2) = 1$ is plotted in dotted line.

Figure 4 : Constraints on the density and the size of the halo of the Local Group from CMB anisotropies. Dotted curves correspond to $y = 2.5 \times 10^{-5}$ (thick), $2.5\times10^{-5}/2$, $2.5\times10^{-5}/4$, $2.5\times10^{-5}/8$, and $2.5\times10^{-5}/16$. Solid curves correspond to $Q_{\mathrm{sz}} = 9\mu\mathrm{K}$, $6\mu\mathrm{K}$ (thick) , $3\mu\mathrm{K}$, $1.5\mu\mathrm{K}$, and $0.75\mu\mathrm{K}$.

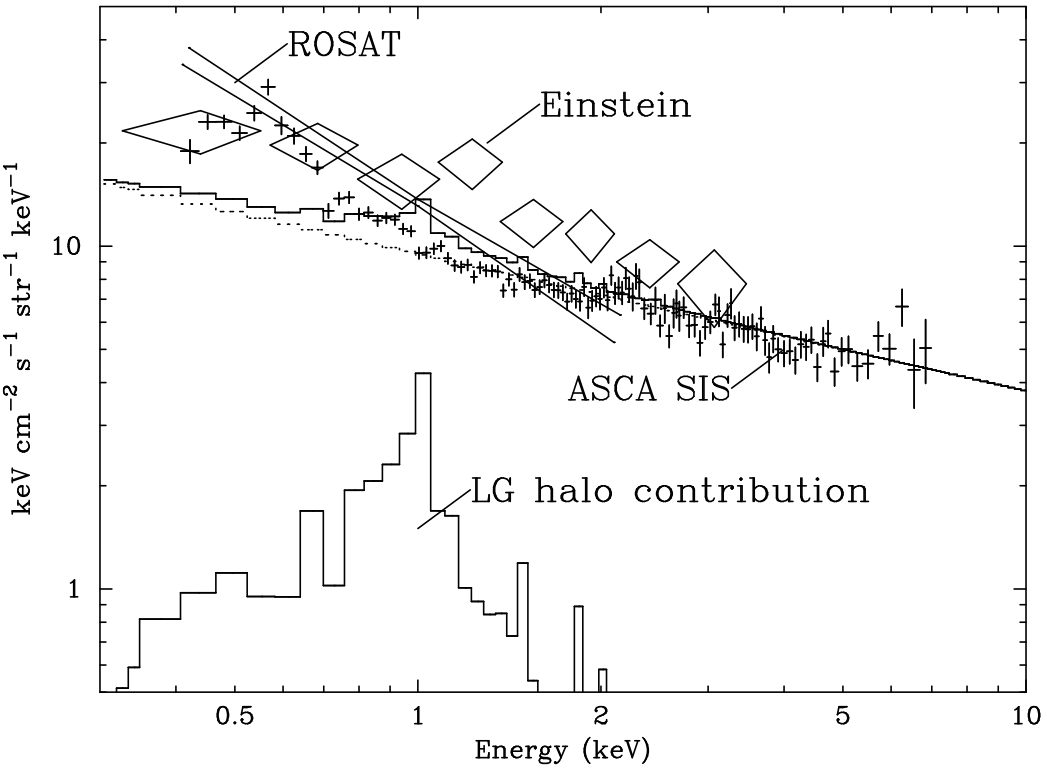

Figure 1: XRB spectra observed with different X-ray satellites. The size of the symbols denote the error bars for ASCA (Gendreau et al. 1995; crosses) and Einstein (Wu et al. 1991; diamonds). The Rosat data (Hasinger 1992) are indicated by the region between the two lines in the upper left. The histogram in the lower left indicates the emission from the X-ray halo of the Local Group with $T = 1\mathrm{keV}$, $r_c = 0.15\mathrm{Mpc}$, $n_0 = 10^{-4}\mathrm{cm}^{-3}$ and 0.3 times solar abundances observed at the center of the LG (computed with the Raymond-Smith model). This LG halo model has a total X-ray luminosity of $10^{41}\mathrm{erg}\cdot\mathrm{s}^{-1}$ between 0.5keV and 4keV, and an electron column density of $6\times10^{20}\mathrm{cm}^{-2}$. The single power-law component extrapolated from the higher energy band, $I(\varepsilon) = 9.6\varepsilon^{-0.4}\mathrm{keV}\cdot\mathrm{s}^{-1}\cdot\mathrm{sr}^{-1}\cdot\mathrm{keV}^{-1}$, is plotted in the dotted line, while the overall prediction (the Local Group emission plus the power-law component) is plotted in the solid line. The Galactic absorption is not taken into account.

Figure 2: Assumed geometry of the X-ray halo of the Local Group.

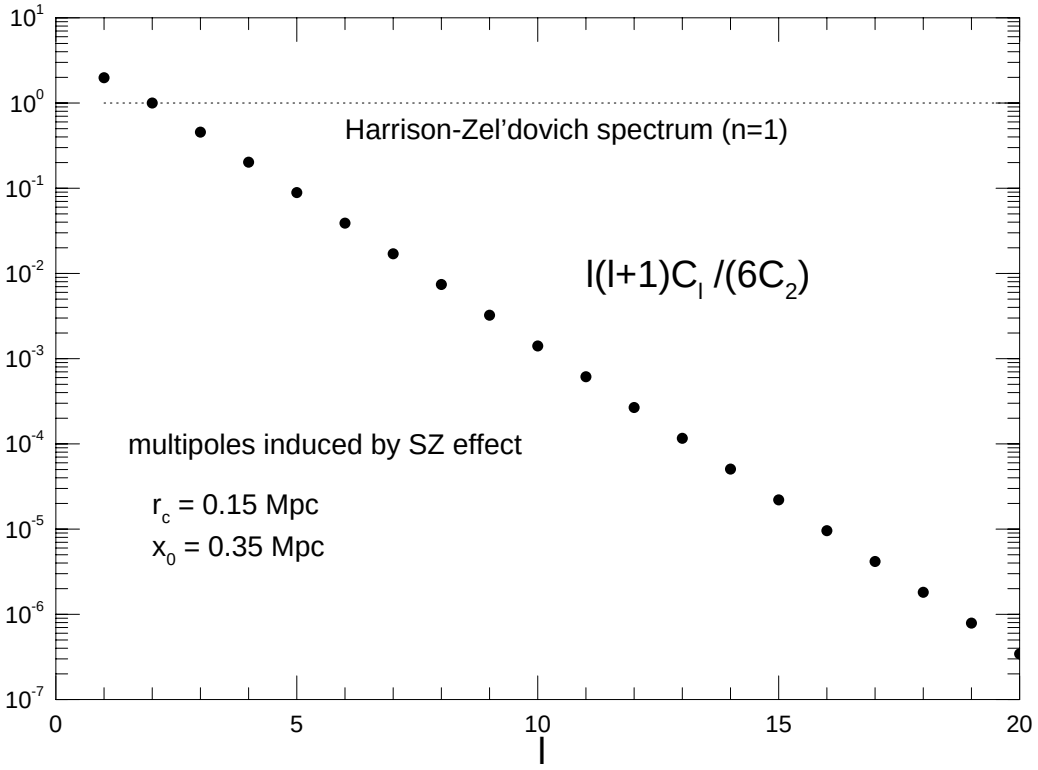

Figure 3: Multipoles induced by the Sunyaev-Zel'dovich effect of the Local Group halo. The primordial Harrison-Zel'dovich spectrum prediction $l(l+1)C_l/(6C_2) = 1$ is plotted in dotted line.

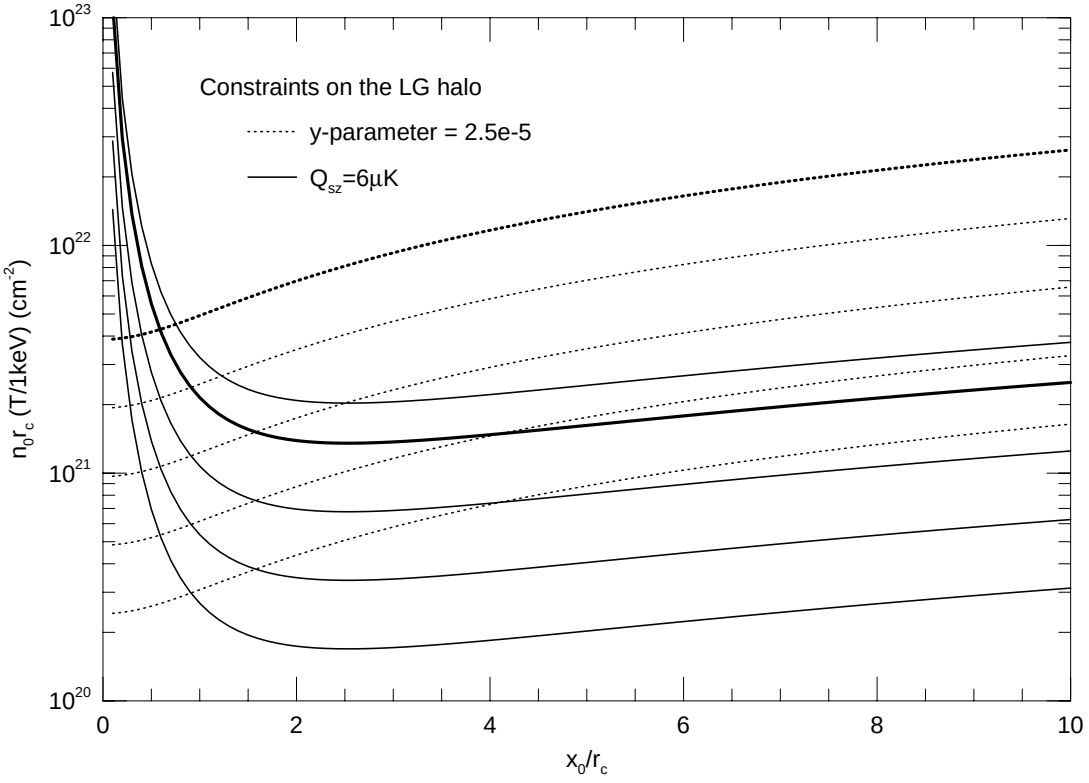

Figure 4: Constraints on the density and the size of the halo of the Local Group from CMB anisotropies. Dotted curves correspond to $y = 2.5 \times 10^{-5}$ (thick), $2.5 \times 10^{-5}/2$, $2.5 \times 10^{-5}/4$, $2.5 \times 10^{-5}/8$, and $2.5 \times 10^{-5}/16$. Solid curves correspond to $Q_{\rm sz} = 9\mu$K , 6μK (thick) , 3μK , 1.5μK , and 0.75μK.